4-1991

An Improved Method for Online Calculation and Compensation of the Static Deflection at a Robot End-Effector

Paul P. Lin
Cleveland State University, p.lin@csuohio.edu

Hsiang-Dih Chiang
Cleveland State University

Xiu Xun Cui
Cleveland State University

Publisher's Statement

This is the accepted version of the following article: Lin, P. P., Hsiang-Dih, C., & Xiu Xun, C. (1991). An Improved Method for On-Line Calculation and Compensation of the Static Deflection at a Robot End-Effector. Journal Of Robotic Systems, 8(2), 267-288. ., which has been published in final form at http://onlinelibrary.wiley.com/doi/10.1002/rob.4620080208/abstract

Original Citation

Lin, P. P., Hsiang-Dih, C., & Xiu Xun, C. (1991). An Improved Method for On-Line Calculation and Compensation of the Static Deflection at a Robot End-Effector. Journal Of Robotic Systems, 8(2), 267-288. .

An Improved Method for On-Line Calculation and Compensation of the Static Deflection at a Robot End-Effector

Paul P. Lin, Hsiang-Dih Chiang, and Xiu Xun Cui
Mechanical Engineering Department
Cleveland State University
Cleveland, OH 44115

INTRODUCTION

A robot with no load at its end-effector may be properly calibrated. When it carries an object of a certain weight moving from one pose (position and orientation) to another, a significant discrepancy exists between the desired and actual pose of the robot. For a light-weight robot manipulator, link deflection is the primary cause of the discrepancy. Due to the distributed weights of robotic links and a load applied at the end-effector, each robotic link and joint are deflected. There have been some researchers on the elastic deflections of robotic manipulators.

Whitney[1] started the pioneering work on the deflection and vibration of jointed beams. Derby[2] developed a first-order compensation analysis for link deflections. The analysis was based on the assumptions of small bending and no radical difference in the deformed arm geometry. Zalucky and Hardt[3] proposed a solution to actively control the deflection using a straightness servo. The system employed two parallel beams, one is to act as the manipulator link and the other one is to carry only the bending loads. Maghdari and Shahinpoor[4] conducted a series of experiments of a PUMA 560 robot manipulator to determine the characteristics of its elastic deformations in various geometrical configurations and modes of operations using a dial gauge with a resolution of 0.001 inch. Fenton and Reeder[5] also developed an elastic deflection compensating algorithm, in which the method they used in solving for the inverse kinematics of a deflected manipulator was analogous to the method of solving for the inverse kinematics of a rigid manipulator. Tang and Wang[6] used a classical beam theory to compute the linear displacements of robotic links and considered the robot joints as torsional springs, where the first order approximation is applied for compliance analysis.

Whitney et al.[7] pointed out five causes of robotic positioning errors. They are backlash, gear transmission error, joint drive compliance, cross coupling of joint rotations, and base motion. The first two are due to manufacturing errors, whereas the third one is the overall compliance between the angular encoder and the actual angular output. When a robot is loaded at its end-effector, couple moments in addition to the driving torques are applied to the joints causing additional angular displacements (i.e., angular deflections). The classical Timoshenko's beam theory has been employed to calculate the slope angle (angular deflection) at the end of each robotic link by researchers such as Derby,[2] Tang and Wang,[6] and Fenton and Reeder.[5] The formula which they used for the calculations was based on a cantilever beam assumption (one end is free and the other end built-in or fixed to a rigid wall). However, all robotic joints, except the first one, are not rigidly fixed. Even for the first joint where a fixed pivot is located, an angular deflection is allowed.

To overcome the problem, this article presents a more accurate way to calculate the angular deflections of robotic joints using one of energy methods. Different methods used to calculate the link deflection of a planar two-link robot made up of aluminum alloy are presented. Experimental data is provided to verify the calculations. An algorithm for compensating a robot end-effector's pose error is developed thereafter. This article presents an improved method for on-line calculation and compensation of the static deflection at a robot end-effector rather than an attempt to reach the accuracy available from a finite element technique.

TRANSFORMATION OF FORCES AND DISPLACEMENTS

Each link of a robotic manipulator may be acted upon by concentrated forces, distributed forces and moments. It is necessary to transform a generalized force vector from one coordinate into another. Here the generalized force vector is a vector which contains three force components and three moment components. Three unit vectors are used to describe the robot end-effector's orientation. They are the approach vector **a** from which the end-effector will approach an object, the orientation vector **o** from fingertip to fingertip, and the normal vector **n** where $\mathbf{n} = \mathbf{o} \times \mathbf{a}$. In addition, a position vector p is used to describe the position of the end-effector with respect to base frame. Paul[8] has developed a method to transform static forces and moments between different coordinate frames. The virtual work W resulting from the application of a generalized force F causing a generalized displacement D is

$$W = F^T D \tag{1}$$

If the same displacement were caused by another force and moment acting at some different points on the object, described by a coordinate frame C, then the same virtual work would result.

$$W = ({}^cF)^T \, {}^cD \tag{2}$$

or

$$F^T D = ({}^cF)^T \, {}^cD \tag{3}$$

Considering that

$${}^cD = {}^0J_c D \tag{4}$$

which is

$$\begin{bmatrix} {}^c\mathbf{d}_x \\ {}^c\mathbf{d}_y \\ {}^c\mathbf{d}_z \\ {}^c\delta_x \\ {}^c\delta_y \\ {}^c\delta_z \end{bmatrix} = \begin{bmatrix} n_x & n_y & n_z & (\mathbf{p} \times \mathbf{n})_x & (\mathbf{p} \times \mathbf{n})_y & (\mathbf{p} \times \mathbf{n})_z \\ o_x & o_y & o_z & (\mathbf{p} \times \mathbf{o})_x & (\mathbf{p} \times \mathbf{o})_y & (\mathbf{p} \times \mathbf{o})_z \\ a_x & a_y & a_z & (\mathbf{p} \times \mathbf{a})_x & (\mathbf{p} \times \mathbf{a})_y & (\mathbf{p} \times \mathbf{a})_z \\ 0 & 0 & 0 & n_x & n_y & n_z \\ 0 & 0 & 0 & o_x & o_y & o_z \\ 0 & 0 & 0 & a_x & a_y & a_z \end{bmatrix} \begin{bmatrix} \mathbf{d}_x \\ \mathbf{d}_y \\ \mathbf{d}_z \\ \delta_x \\ \delta_y \\ \delta_z \end{bmatrix} \tag{5}$$

where J is called the Pose Jacobian matrix and ${}^0J_c$ denotes the Pose Jacobian of frame C with respect to base frame. Using eqs. (3) and (4), gives

$$F = ({}^0J_c)^T\, {}^cF \tag{6}$$

that is

$$\begin{bmatrix} f_x \\ f_y \\ f_z \\ m_x \\ m_y \\ m_z \end{bmatrix} = \begin{bmatrix} n_x & o_x & a_x & 0 & 0 & 0 \\ n_y & o_y & a_y & 0 & 0 & 0 \\ n_z & o_z & a_z & 0 & 0 & 0 \\ (\mathbf{p}\times\mathbf{n})_x & (\mathbf{p}\times\mathbf{o})_x & (\mathbf{p}\times\mathbf{a})_x & n_x & o_x & a_x \\ (\mathbf{p}\times\mathbf{n})_y & (\mathbf{p}\times\mathbf{o})_y & (\mathbf{p}\times\mathbf{a})_y & n_y & o_y & a_y \\ (\mathbf{p}\times\mathbf{n})_z & (\mathbf{p}\times\mathbf{o})_z & (\mathbf{p}\times\mathbf{a})_z & n_z & o_z & a_z \end{bmatrix} \begin{bmatrix} {}^cf_x \\ {}^cf_y \\ {}^cf_z \\ {}^cm_x \\ {}^cm_y \\ {}^cm_z \end{bmatrix} \tag{7}$$

where F is a generalized force vector described in the base frame.

The distributed force acting upon link n can be considered as a concentrated force acting at the centroid of link n, which can be decomposed into three components with directions consistent with the X, Y, and Z axes of the local frame n. For a robot manipulator subjected to a concentrated load P at the end-effector and distributed forces W acting upon all links, the generalized force vector at coordinate frame i in frame $i-1$ coordinates, is given by

$${}^{i-1}F_i = ({}^{i-1}J_n)^T\, {}^nP_n + \sum_{k=i}^{n} ({}^{i-1}J_{ck})^T\, {}^kW_{ck} \tag{8}$$

where ${}^{i-1}J_n$ is a pose Jacobian describing the coordinate relationship of frame n with respect to frame $i-1$, ${}^{i-1}J_{ck}$ is another pose Jacobian describing the coordinate relationship of the centroid of link k with respect to the origin of frame $i-1$, ${}^nP_n$ is a concentrated force acting at the origin of frame n in frame n coordinates, and ${}^kW_{ck}$ is a distributed force acting at the centroid of link k in frame k coordinates.

For a planar two-link robot as shown in Figure 1 bearing distributed weights W_1 and W_2 on links 1 and 2, respectively, and a concentrated weight P at the end-effector, the generalized forces are given by

$${}^1F_2 = ({}^1J_2)^T\, {}^2P_2 + ({}^1J_{C2})^T\, {}^2W_{c2} \tag{9}$$

$${}^0F_1 = ({}^0J_2)^T\, {}^2P_2 + ({}^0J_{C2})^T\, {}^2W_{c2} + ({}^0J_{C1})^T\, {}^1W_{c1} \tag{10}$$

where ${}^1F_2$ and ${}^0F_1$ are the equivalent generalized force vectors at frame 2 in frame 1 coordinates, and at frame 1 in the base frame coordinates, respectively.

$${}^2P_2 = [-PS_{12} \quad -PC_{12} \quad 0 \quad 0 \quad 0 \quad 0]^T \tag{11}$$

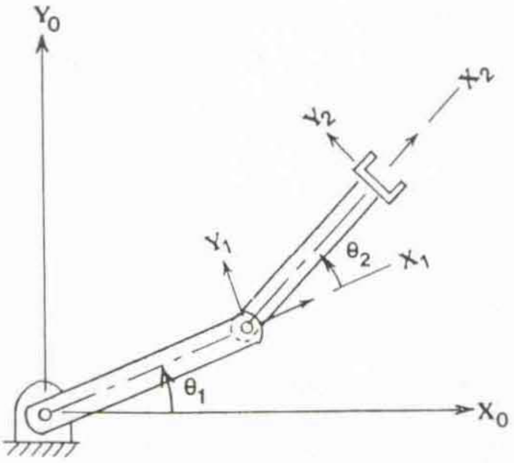

Figure 1. Coordinate frames for the planar two-link robot.

and likewise

$$^{2}W_{c2} = [-W_2L_2S_{12} \quad -W_2L_2C_{12} \quad 0 \quad 0 \quad 0 \quad 0]^T \tag{12}$$

where C_1 = Cosine of θ_1, C_{12} = Cosine of $(\theta_1 + \theta_2)$ and S_{12} = Sine of $(\theta_1 + \theta_2)$, etc., and the superscript $c2$ denotes that the weight W_2 is applied at the centroid of link 2.

A systematic way to derive the above two equations is by means of the so-called A matrix developed by Denavit and Hartenberg.[9] An A matrix is a homogeneous transformation describing the relative translation and rotation between link coordinate systems. Thus, the position and orientation of the second link in the base frame coordinates is given by

$$^{0}T_2 = {}^{0}A_1 \, {}^{1}A_2 \tag{13}$$

that is

$$^{0}T_2 = \begin{pmatrix} C_{12} & -S_{12} & 0 & L_1C_1 + L_2C_{12} \\ S_{12} & C_{12} & 0 & L_1S_1 + L_2S_{12} \\ 0 & 0 & 1 & 0 \\ 0 & 0 & 0 & 1 \end{pmatrix} \tag{14}$$

where the first three elements of the second column represent the Y direction of frame 2 in the base frame coordinates. Inversely, the first three elements of the second row represent the Y direction of the base frame in frame 2 coordinates. Using Jacobian expressions and substituting eqs. (11) and (12) into eq. (9), gives

$$^{1}F_2 = [-PS_1 - W_2L_2S_1 \quad -PC_1 - W_2L_2C_1 \quad 0 \quad 0 \quad 0 \quad -PL_2C_{12} - 0.5W_2L_2^2C_{12}]^T \quad (15)$$

Likewise, the expression for $^{0}F_1$ can be obtained

$$^{0}F_1 = [0 \quad -P - W_2L_2 - W_1L_1 \quad 0 \quad 0 \quad 0 \quad m_z]_T \quad (16)$$

where

$$m_z = -P(L_1C_1 + L_2C_{12}) - 0.5W_1L_1^2C_1 - W_2L_2(L_1C_1 + 0.5L_2C_{12}) \quad (17)$$

The employment of the force transformation between coordinate frames provides a systematic way to calculate the equivalent force vectors. It is important and essential for robotic manipulators with more than two links.

CALCULATIONS OF LINK DEFLECTIONS

Robotic link deflections can be calculated by at least two methods. The Timoshenko's beam theory has been widely used as a classical method. Of equal importance, the Castigliano's second theorem, one of energy methods, is another powerful method. They are briefly described as follows;

Employment of the Timoshenko's Beam Theory

Deflection of a One-Link Robot

In using the Timoshenko's beam theory, a link is treated as a cantilever beam. Four possible loading conditions are shown in Figure 2 in which the total deflection can be easily superimposed for a combined loading condition. The deflection expressions for the four cases are shown as follows[10]

$$d_p = PL^3/3EI \quad (18)$$

$$d_w = WL^4/8EI \quad (19)$$

$$d_m = ML^2/2EI \quad (20)$$

$$d_f = FL/EA \quad (21)$$

Since the deflection due to an axial load is much smaller than others, it is assumed negligible throughout this article. For the planar two-link robot as shown in Figure 1, link 2 is subjected to the concentrated load P and distributed weight W_2 only. The deflections of link 2 (scalar form) in frame 2 coordinates

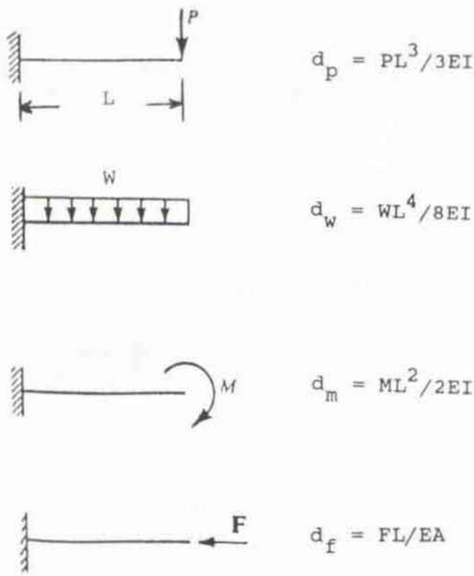

Figure 2. Deflection of a cantilever beam with different loading conditions (Timoshenko's beam theory).

due to P and W_2 can be derived by substituting eqs. (11) and (12) into (18) and (19), respectively.

$$ {}^2d_p = -PC_{12}L_2^3/3E_2I_2 \tag{22} $$

$$ {}^2d_W = -W_2L_2^4C_{12}/8E_2I_2 \tag{23} $$

Deflection of a Multilink Robot via Force and Displacement Transformations

A general methodology based on the Timoshenko's beam theory via force and displacement transformations to calculate the end-effector's deflection of a multilink robot is developed. The differential changes of deflections can be oriented such that the deflection of each link is described in the same frame coordinates (base frame coordinates) by multiplying a matrix, called the Orientation Jacobian, J'.

$$ D = J'\,{}^cD \tag{24} $$

where

$$J' = \begin{pmatrix} n_x & o_x & a_x & 0 & 0 & 0 \\ n_y & o_y & a_y & 0 & 0 & 0 \\ n_z & o_z & a_z & 0 & 0 & 0 \\ 0 & 0 & 0 & n_x & o_x & a_x \\ 0 & 0 & 0 & n_y & o_y & a_y \\ 0 & 0 & 0 & n_z & o_z & a_z \end{pmatrix} \tag{25}$$

and ${}^cD$ is a displacement vector in frame C coordinates. For the robot shown in Figure 1, the deflection of link 2 in base frame coordinates can be expressed as follows:

$${}^0d_2 = ({}^0J_2')\,{}^2d_p + ({}^0J_{C2}')\,{}^2d_{Wc2} \tag{26}$$

where ${}^2d_p$ and ${}^2d_{Wc2}$ are treated as 6×1 column vectors whose nonzero elements are the scalars shown in eqs. (22) and (23), respectively. The Y or vertical component of the deflection is

$$\begin{aligned} {}^0d_{2y} &= -(PL_2^3C_{12}^2/3E_2I_2) - (W_2L_2^4C_{12}^2/8E_2I_2) \\ &= -L_2^3C_{12}^2(8P + 3W_2L_2)/24E_2I_2 \end{aligned} \tag{27}$$

With the addition of a moment effect, the deflection of link 1 can be derived in a similar way, whose y component is

$$\begin{aligned} {}^0d_{1y} = -(&8PL_1^3C_1^2 + 12PL_1^2L_2C_1C_{12} + 8W_2L_1^3L_2C_1^3 \\ &+ 6W_2L_1^2L_2^2C_1C_{12} + 3W_1L_1^4C_1^2)/24E_1I_1 \end{aligned} \tag{28}$$

Finally, the vertical deflection of the end-effector of the two-link robot in base frame coordinates is given by

$${}^0d = {}^0d_{1y} + {}^0d_{2y} \tag{29}$$

Employment of the Castigliano's Second Theorem

There are two theorems due to Castigliano. The Castigliano's second theorem[11] is stated as follows:

$$\partial Y = \partial U/\partial P \tag{30}$$

where U is strain energy, Y is the displacement in the direction and, at the point of application, of an applied force P.

In applying the Castigliano's second theorem, the strain energy must be expressed as a function of the load. A straight beam or link may be subjected to a number of common loads such as axial force, bending moment, shear force and twisting moment. For the planar two-link robot, it is mainly subjected to bending moments M only. Axial and shear forces are assumed negligible and there is no twisting moment in this case. The strain energy is reduced to the following

$$U = \int \frac{M^2}{2EI}\,dx \tag{31}$$

where the integration is carried out over the length of the link. Accordingly, the vertical deflection (downward) at the end-effector is

$$\begin{aligned} Y = &-L_2^3C_{12}^2(8P + 3W_2L_2)/24E_2I_2 \\ &- [PL_1(8L_1^2C_1^2 + 24L_1L_2C_1C_{12} + 24L_2^2C_{12}^2) \\ &+ W_2L_1L_2(8L_1^2C_1^2 + 18L_1L_2C_1C_{12} + 12L_2^2C_{12}^2) \\ &+ W_1L_1^3(3L_1C_1^2 + 4L_2C_1C_{12})]/24E_1I_1 \end{aligned} \tag{32}$$

where P is the applied load and

E_1, E_2: modulus of elasticity of links 1 and 2, respectively
I_1, I_2: area moment of inertia of links 1 and 2, respectively
L_1, L_2: length of links 1 and 2, respectively

Comparison between Two Methods

Comparing eq. (32) with eq. (29), the difference in deflection is quite substantial. The eq. (32) contains more terms which will likely result in a higher value of deflection. The comparison between these two methods is shown in Table II. It should be noted that there is absolutely no difference in deflection between these two methods for a one-link robot as shown in Table I.

Table I. Difference in calculated deflections between two methods for a one-link robot with one revolute joint. The robot data is as follows: Link length: 24 inches, Moment of inertia: 1.920 in.^{4}, Modulus of elasticity: 10E +6 psi. Load P = 3.05 lb is applied at the robot end-effector, YC: Vertical deflection using the Castigliano's second theorem, YT: Vertical deflection using the Timoshenko's beam theory.[a]

Theta1 (deg.)	YC (in.)	YT (in.)
0	0.00122	0.00122
20	0.00107	0.00107
40	0.00071	0.00071
60	0.00030	0.00030
80	0.00004	0.00004

[a] The American Customary Unit System (inch-pound) is used throughout this paper since the experimental data (listed in Table III) was obtained using a dial gage with a resolution of 0.001 inch. 1 lb = 0.454 kg and inch = 25.4 mm in the SI Unit System. Angle theta1 is with respect to the horizontal x axis of the base frame.

Table II. Difference in calculated deflections between two methods for a planar two-link robot with two revolute joints. The robot data is as follows: Length of link 1: 24 inches (uniform hollow square cross section), Length of link 2: 24 inches (uniform hollow square cross section), Area moment of inertia of link 1: 1.920 in.[4], Area moment of inertia of link 2: 0.289 in.[4], Modulus of elasticity of link 1: 10E + 6 psi (aluminum alloy), Modulus of elasticity of link 2: 10E + 6 psi (aluminum alloy). Load P = 3.05 lb is applied at the end-effector, YC: vertical deflection calculated using the Castigliano's second theorem, YT: vertical deflection calculated using the Timoshenko's beam theory, PTG: $|(YT - YC)/YC| \times 100$.

Theta1 (deg.)	Theta2 (deg.)	YC (in.)	YT (in.)	PTG (%)
0.0	0.0	0.01523	0.00959	37.03
0.0	22.5	0.01356	0.00856	36.88
0.0	90.00	0.00179	0.00179	0.0
22.5	−22.5	0.01466	0.00921	37.18
22.5	−45.0	0.01300	0.00819	37.00
22.5	67.5	0.00152	0.00152	0.00
45.0	0.0	0.00762	0.00480	37.00
45.0	−45.0	0.01313	0.00825	37.17
45.0	−67.5	0.01154	0.00725	37.18
67.5	−22.5	000604	0.00381	36.84
67.5	−45.0	0.00969	0.00616	36.36
90.0	−22.5	0.00137	0.00092	32.85
90.0	−45.0	0.00466	0.00314	32.62

[a] The uniformly distributed weights of links 1 and 2 are considered. Theta1 is the angle of link 1 with respect to the horizontal axis of the base frame and theta2 is the relative angle from link 1 to link 2. For the purpose of comparison, the additional link deflections resulting from angular deflections of joints 1 and 2 are not considered in the above calculations.

Tang and Wang[6] gave a two-link robot as a numerical example and compared the theoretical calculations of link deflections using a classical beam theory and the Castigliano's second theorem. Their study showed that the two calculations were quite close to each other. The reason is that the rotational axes of the robotic links are perpendicular to each other and the first link always stands up vertically. This means that link 1 is almost undeflected when a weight is applied vertically at the end of the second link. Thus, their example was essentially to illustrate the calculated deflections of a one-link robot using two different methods. In addition, the Castigliano's second theorem which they used was solely for calculating the link deflections. The angular deflections of robotic joints were ignored in their calculations.

ADDITIONAL LINK DEFLECTIONS RESULTING FROM ANGULAR DEFLECTIONS

Calculation of Angular Deflections Using the Castigliano's Second Theorem

Figure 3 shows that the total vertical deflection dy comprises two parts, d_{y1} and d_{y2}, where d_{y1} is the additional vertical deflection resulting from an angular

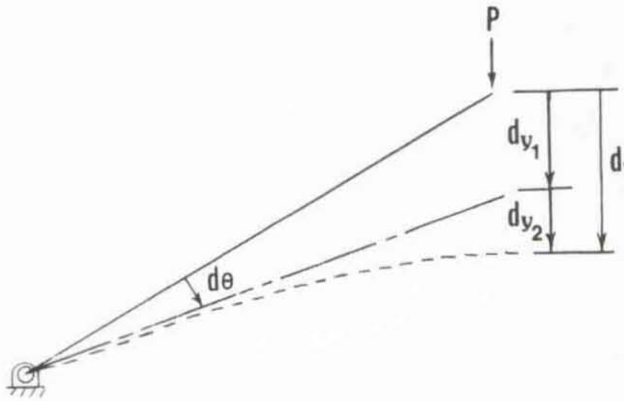

Figure 3. Deflection of a one-link robot with a revolute joint.

deflection $d\theta$ due to an applied couple moment, and d_{y2} is the vertical deflection resulting from a concentrated load P at the end-effector. Traditionally, a robot manipulator has been treated as a series of cantilever beams in order to perform the deflection analysis. The basic assumption when employing the classical beam theory is that a joint is considered rigidly fixed to a wall where the angular and linear deflections are disallowed. This conflicts with the reality that all robotic joints, except the first one, are not rigidly fixed to a stationary foundation. Besides, even for the first one, a small angular deflection is still possible.

The Castigliano's second theorem can be used to calculate link deflections or angular deflections. For a link subjected to an applied coupled (bending or twisting) moment C, the rotational angle of twist (angular deflection) at a specific point is given by[11]

$$\theta_i = \partial U / \partial C_i \tag{33}$$

where U is strain energy. Considering a link subjected to a bending moment only, the expression for the angle of rotation (or the angular deflection) is

$$\theta = \frac{1}{EI} \int M \frac{\partial M}{\partial C}\, dx \tag{34}$$

For a planar two-link robot when a load P is applied at the end-effector and the weights of links, W_1 and W_2 are considered, the angular deflection of joint 2 can be easily calculated using eq. (34). The calculation of the angular deflection of joint 1, however, requires the employment of a fictive bending moment at the origin of the base frame. The fictive moment will be set to zero later.

$$d\theta_1 = -(A/E_1 I_1) - (B/E_2 I_2) \tag{35}$$

where

$$A = PL_1(L_2C_{12} + L_1C_1/2) + W_1L_1^3C_1/6 + W_2L_1L_2(L_1C_1 + L_2C_{12})/2$$
$$B = PC_{12}L_2^2/2 + W_2L_2^3C_{12}/6$$

Likewise,

$$d\theta_2 = -B/E_2I_2 \tag{36}$$

It is worthwhile to note that if the Timoshenko's beam theory were employed, $d\theta_2$ would be the same but $d\theta_1$ would be always zero. The difference is very obvious.

Calculation of Additional Link Deflections Resulting from Angular Deflections

Since angular deflections are small, they can be considered as joint differential changes. Employing the concepts of differential relationships, the additional link deflections resulting from angular deflections can be more easily and systematically calculated. For a six-link robot, the differential changes in the position and orientation of a T_6 matrix are caused by differential changes in joint coordinates. In the case of a revolute joint, dq_i corresponds to a differential rotation, and in the case of a prismatic joint, dq_i corresponds to a differential change in the joint distance.

Paul[8] has derived the differential change as a function of six joint coordinates written as a six-by-six matrix consisting of differential rotation and translation vector elements. Each column of the Jacobian consists of the differential translation and rotation vectors corresponding to the differential changes of each of the joint coordinate.

$$\begin{bmatrix} T_{6d_x} \\ T_{6d_y} \\ T_{6d_z} \\ T_{6\delta_x} \\ T_{6\delta_y} \\ T_{6\delta_z} \end{bmatrix} = \begin{bmatrix} T_{6d_{1x}} & T_{6d_{2x}} & T_{6d_{3x}} & T_{6d_{4x}} & T_{6d_{5x}} & T_{6d_{6x}} \\ T_{6d_{1y}} & T_{6d_{2y}} & T_{6d_{3y}} & T_{6d_{4y}} & T_{6d_{5y}} & T_{6d_{6y}} \\ T_{6d_{1z}} & T_{6d_{2z}} & T_{6d_{3z}} & T_{6d_{4z}} & T_{6d_{5z}} & T_{6d_{6z}} \\ T_{6\delta_{1x}} & T_{6\delta_{2x}} & T_{6\delta_{3x}} & T_{6\delta_{4x}} & T_{6\delta_{5x}} & T_{6\delta_{6x}} \\ T_{6\delta_{1y}} & T_{6\delta_{2y}} & T_{6\delta_{3y}} & T_{6\delta_{4y}} & T_{6\delta_{5y}} & T_{6\delta_{6y}} \\ T_{6\delta_{1z}} & T_{6\delta_{2z}} & T_{6\delta_{3z}} & T_{6\delta_{4z}} & T_{6\delta_{5z}} & T_{6\delta_{6z}} \end{bmatrix} \begin{bmatrix} dq_1 \\ dq_2 \\ dq_3 \\ dq_4 \\ dq_5 \\ dq_6 \end{bmatrix} \tag{37}$$

where the first matrix on the right-hand side is called the Differential Jacobian J''. If joint i is revolute, then

$$T_{6d_i} = (-n_xp_y + n_yp_x)i + (-o_xp_y + o_yp_x)j + (a_xp_y + a_yp_x)k \tag{38}$$

$$T_{6\delta_i} = n_zi + o_zj + a_zk \tag{39}$$

If joint i is prismatic, then

$$T_{6d_i} = n_z i + o_z j + a_z k \tag{40}$$

$$T_{6\delta_i} = 0i + 0j + 0k \tag{41}$$

Thus, for the given two-link robot, the end-effector's deflection vector in terms of frame 2 coordinates is expressed by

$$[{}^2d] = J''[d\theta] \tag{42}$$

where the Differential Jacobian J'' is

$$J'' = \begin{pmatrix} L_1S_2 & 0 \\ L_2 + L_1C_2 & L_2 \\ 0 & 0 \\ 0 & 0 \\ 0 & 0 \\ 1 & 1 \end{pmatrix} \tag{43}$$

Thus,

$$\begin{pmatrix} {}^2d_x \\ {}^2d_y \\ {}^2d_z \\ {}^2\delta_x \\ {}^2\delta_y \\ {}^2\delta_z \end{pmatrix} = \begin{pmatrix} L_1S_2d\theta_1 \\ L_1C_2d\theta_1 + L_2(d\theta_1 + d\theta_2) \\ 0 \\ 0 \\ 0 \\ d\theta_1 + d\theta_2 \end{pmatrix} \tag{44}$$

In order to sum deflections of different links, deflection vectors are oriented such that they are all referred to the same coordinates which are the base frame coordinates. It should be noted that the deflections are not transformed back to the base frame. They are still located at the end of each link. The deflection of link 2 in terms of the base frame coordinates can be obtained by premultiplying the above deflection vector, eq. (44) by the Orientation Jacobian, J' in eq. (25). Thus,

$$\begin{pmatrix} d_x \\ d_y \\ d_z \\ \delta_x \\ \delta_y \\ \delta_z \end{pmatrix} = \begin{pmatrix} -L_1S_1d\theta_1 - L_2S_{12}(d\theta_1 + d\theta_2) \\ L_1C_1d\theta_1 - L_2C_{12}(d\theta_1 + d\theta_2) \\ 0 \\ 0 \\ 0 \\ d\theta_1 + d\theta_2 \end{pmatrix} \tag{45}$$

Since the concentrated load P and distributed weights W_1 and W_2 are all in the negative y direction of the base frame coordinates, d_y is the most significant component among the six elements of the displacement vector at the end-effector.

$$\begin{aligned} {}^0d_y &= L_1C_1d\theta_1 + L_2C_{12}(d\theta_1 + d\theta_2) \\ &= -A(L_1C_1 + L_2C_{12})/E_1I_1 - B(L_1C_1 + 2L_2C_{12})/E_2I_2 \end{aligned} \tag{46}$$

where A and B were defined in eq. (36). Finally, the total deflection at the end-effector of the given two-link robot is the sum of the link deflection, ${}^0d$ and the additional link deflection resulting from the angular deflections of joints, ${}^0d_y$.

$${}^0d_{\text{total}} = {}^0d + {}^0d_y \tag{47}$$

where ${}^0d$ is from eq. (29) and ${}^0d_y$ is from eq. (46).

EXPERIMENT

To verify the theoretical deflection analysis, a planar two-link robot was built. It was made up of light-weight aluminum alloy. The robot data is as follows:

- Length of link 1: 24 inches (uniform hollow square cross section)
- Length of link 2: 24 inches (uniform hollow square cross section)
- Area moment of inertia of link 1: 1.920 in.^{4}
- Area moment of inertia of link 2: 0.289 in.^{4}
- Modulus of elasticity of link 1: 10E + 6 psi
- Modulus of elasticity of link 2: 10E + 6 psi

To exclude the possibilities of gear backlash, gear transmission error, joint drive compliance, and cross coupling of joint rotations, the robotic joints are mechanical pin joints with no actuators. The robot was designed to have a finite rotational increment of 22.5 degrees, which was accomplished by locating a pin in a different pin hole. To avoid a possible rotational slippage of a joint, two set screws were used to fix the joint at a specified angular position. Various weights could be applied at the end-effector. A dial gauge of 0.001 inch (0.0254 mm) resolution was used to measure the end-effector's deflection after a weight has been applied. The procedure was repeated until all possible arm configurations and applied weights had been tested.

Table III shows a comparison between theoretical calculations and experimental data. As can be seen, the theoretical calculation YCD or YTD is generally in agreement with the experimental data. Notice that YD (the vertical deflection resulting from the angular deflections of all joints) is the most dominant factor. It is much greater than YC or YT.

Table III. Comparison of deflections between theoretical calculations and experimental data. The robot data is the same as in Table I. Load P = 1.02 lb is applied at the end-effector. YC: vertical deflection calculated using the Castigliano's second theorem, YT: vertical deflection calculated using the Timoshenko's beam theory, YD: vertical deflection resulting from the angular deflections of all joints, YTD = YT + YD, YCD = YC + YD, EXP: Experimental data (vertical deflections at the end-effector are measured using a dial gauge with a resolution of 0.001 inch after a weight of 1.02 lb has been applied at the end-effector).

Theta1 (deg.)	Theta2 (deg.)	YC (in.)	YT (in.)	YD (in.)	YTD (in.)	YCD (in.)	EXP (in.)
0.0	0.0	0.0033	0.0022	0.0095	0.0118	0.0128	0.0150
0.0	22.5	0.0029	0.0020	0.0084	0.0104	0.0113	0.0140
22.5	−22.5	0.0032	0.0022	0.0092	0.0114	0.0124	0.0130
22.5	−45.0	0.0029	0.0019	0.0081	0.0100	0.0110	0.0120
45.0	0.0	0.0017	0.0011	0.0048	0.0059	0.0065	0.0060
45.0	−22.5	0.0026	0.0018	0.0073	0.0090	0.0099	0.0110
45.0	−45.0	0.0030	0.0020	0.0083	0.0103	0.0113	0.0100
45.0	−67.5	0.0026	0.0018	0.0073	0.0090	0.0099	0.0090
67.5	−22.5	0.0014	0.0009	0.0038	0.0048	0.0052	0.0050
67.5	−45.0	0.0023	0.0016	0.0061	0.0077	0.0084	0.0070
90.0	−22.5	0.0003	0.0002	0.0008	0.0010	0.0011	0.0010
90.0	−45.0	0.0012	0.0008	0.0028	0.0036	0.0040	0.0040

[a] Two robotic links are predeflected due to their distributed weights before a load is applied at the end-effector. The dial gauge used to measure the deflections is zeroed after the robot has been predeflected. In order to compare the calculated deflections with the measured ones, the distributed weights W_1 and W_2 are not included in the theoretical calculations.

METHODOLOGY OF DEFLECTION ANALYSIS AND COMPENSATION ALGORITHM FOR A SIX DEGREE-OF-FREEDOM ELBOW MANIPULATOR

As a further example of the deflection analysis a six-degree-of-freedom elbow manipulator containing only revolute joints is investigated. The robot manipulator is made of aluminum alloy whose coordinate frames are shown in Figure 4 and link parameters are described in Table IV,[8] where α is the twist angle between two consecutive rotational axes, a is the common normal distance between two consecutive rotational axes, and d is the distance along the

Table IV. Link parameters of robot manipulator.

Link	Variable	α (degree)	a (in.)	d (in.)
1	theta1	90	0	0
2	theta2	0	24	0
3	theta3	0	24	0
4	theta4	−90	10	0
5	theta5	90	0	0
6	theta6	0	0	3.5

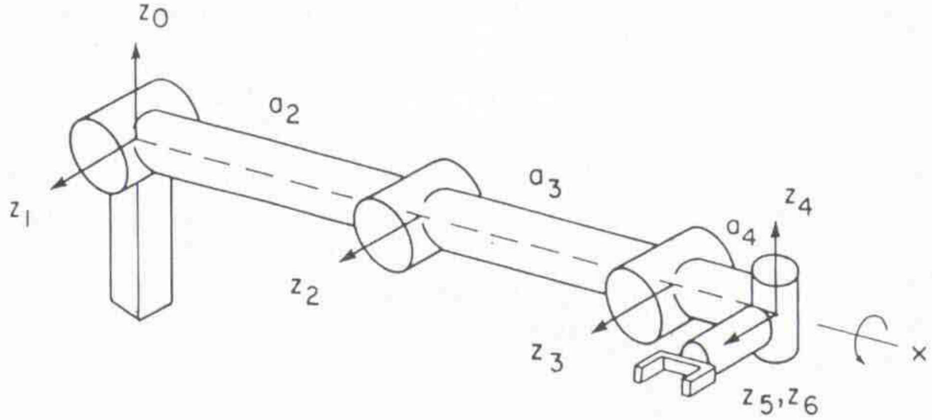

Figure 4. Coordinate frames for the elbow manipulator.

rotational axis between two links. The variables are joint angles theta1 through theta5. It is assumed that the robot manipulator has constant hollow circular cross sections whose outside and inside diameters are 2.0 and 1.8 inches, respectively.

The procedure along with numerical data is as follows:

Input data:

The applied load P is 5.0 lb (2.27 kg).
The desired pose matrix (i.e., T_6) is

$$\begin{pmatrix} 1 & 0 & 0 & 15 \\ 0 & 1 & 0 & 20 \\ 0 & 0 & 1 & 10 \\ 0 & 0 & 0 & 1 \end{pmatrix}$$

Step 1: Transform forces and moments from the end-effector to each joint through the pose Jacobian matrix described in eq. (8).

Step 2: Calculate the deflection of each link using the Timoshenko's beam theory.

Step 3: Apply the Castigliano's second theorem, one of energy methods, to calculate the angular deflections of joints.

Step 4: Calculate the additional link deflections resulting from the angular deflections.

Step 5: Use a 6 × 6 transformation matrix (orientation Jacobian) to orient all the link deflections into the same coordinates which are the base frame coordinates. Finally, the total deflection is formed by summing all local deflections.

Table V. Deflections for different arm configurations.

Theta 1 (deg.)	Theta 2 (deg.)	Theta 3 (deg.)	Theta 4 (deg.)	Theta 5 (deg.)	Theta 6 (deg.)	Deflection (in.)	
53.130	58.612	−117.224	148.612	90.000	−143.130	.00329	(1)
53.130	−58.612	117.224	31.388	90.000	−143.130	.00703	(2)
53.130	86.824	−96.329	279.505	−90.000	36.870	.01538	(3)
53.130	−9.505	96.329	183.176	−90.000	36.870	.05824	(4)
233.130	−121.388	−117.224	328.612	90.000	36.870	.00686	(5)
233.130	121.388	117.224	−148.612	90.000	36.870	.00313	(6)
233.130	−170.495	−96.329	176.824	−90.000	−143.130	.05828	(7)
233.130	93.176	96.329	80.495	−90.000	−143.130	.01542	(8)

Step 6: Compute the total deflection by adding the additional link deflection calculated in step 4 to the link deflection calculated in step 2.

Step 7: Compute the inverse joint solutions of all possible arm configurations and their vertical deflections. Due to the kinematic design of the given robot manipulator, there exists eight possible arm configurations which are listed in Table V.

Step 8: Use a bubble sorting technique to select the optimum arm configuration which has the smallest deflection. The smallest end-effector's deflection selected is .00313 inches and the six joint angles are

Theta 1	Theta 2	Theta 3	Theta 4	Theta 5	Theta 6
233.130	121.388	117.224	−148.612	90.000	36.870

Step 9: Using the concepts of differential relationships and the inverse of the Differential Jacobian, the 6×1 total deflection vector in Cartesian space is transformed to a 6×1 angular deflection vector in joint space, which is listed as follows:

$$
\begin{aligned}
\text{Add\_1} &= 0.0043 \text{ deg.} \\
\text{Add\_2} &= 0.0035 \text{ deg.} \\
\text{Add\_3} &= -0.0070 \text{ deg.} \\
\text{Add\_4} &= 0.0035 \text{ deg.} \\
\text{Add\_5} &= 0.0000 \text{ deg.} \\
\text{Add\_6} &= -0.0043 \text{ deg.}
\end{aligned}
$$

Step 10: Compensate the end-effector's deflection by subtracting the above angles from the original joint angles. The angles in degrees before and after the compensation are listed in Table VI.

The calculated static deflection at the end-effector after the compensation is theoretically zero. Consequently, the position and orientation of the end-effec-

Table VI. Angles in degrees before and after compensation.

Joint	Before Compensation	After Compensation
1	233.1301	233.1258
2	121.3882	121.3847
3	117.2237	117.2307
4	−148.6118	−148.6153
5	90.0000	90.0000
6	36.8699	36.8742

tor theoretically remain the same as the desired ones. The total deflection d_y at the end-effector of the Elbow Manipulator is derived and shown in the Appendix.

DISCUSSIONS

In this work, the Castigliano's second theorem (one of energy methods) is used to calculate link deflections and angular deflections. Table I shows a comparison of calculated deflections at the end-effector of a one-link robot between using the Timoshenko's beam theory and the Castigliano's second theorem. There is no difference in deflection between them for a one-link robot. The difference becomes more obvious when the number of links increases. For a planar two-link robot, the difference is over 30% as shown in Table II.

This study shows that the most contributory factor to the end-effector's total deflection is the additional link deflections resulting from the angular deflections of joints. To more accurately calculate the angular deflections, the Castigliano's second theorem is employed. Table III shows a comparison of the end-effector's deflections for a planar two-link robot between theoretical calculations and experimental data. When the additional link deflection YD is added to the either *YT* or *YC* where *YT* and *YC* are the vertical deflections using the Timoshenko's beam theory and the Castigliano's second theorem, respectively, the resultant deflection becomes reasonably close to the experimental data. This can be reasoned that the use of an energy method should result in a more accurate calculation of link deflection. Since the additional link deflection *YD* as shown in Table III is much larger than either *YT* or *YC*, the total deflections calculated by $YTD = YT + YD$ or $YCD = YC + YD$ are approximately the same. For a six-degree-of-freedom robot such as the elbow manipulator, it is extremely tedious to derive the expression for the end-effector's deflection using the Castigliano's second theorem. Hence, the Timoshenko's beam theory is used to calculate the link deflection at the end of each link individually.

This article presents a systematic approach to calculating deflections through three different Jacobians. The first one is called the "Pose Jacobian," which is used for transformation of forces between coordinate frames. The second one is called the "Orientation Jacobian," which is used to orient a deflection vector from a local frame to the base frame. The local deflection is not transformed back to the origin of the base frame. It stays at the end of a link so that the magnitude of the deflection can remain the same. The purpose of using the orientation Jacobian is to sum the deflections of all links if they are all with respect to the base frame coordinates. The third one is called the "Differential Jacobian." It is written as a 6×6 matrix consisting of differential rotation and translation vector elements. The multiplication of the Jacobian and a vector consisting of differential joint displacement changes gives the differential changes in position and orientation of the end-effector. This concept is used to calculate the additional link deflections resulting from angular deflections. The additional deflections are then added to the link deflections which are calculated using the Timoshenko's beam theory. The total deflection at the end-effector is finally transformed from Cartesian space to joint space by inverting the differential Jacobian.

The concept of differential relationships, especially the use of the differential Jacobian allows us to gracefully perform a transformation of differential changes between Cartesian space and joint space. Based on the differential joint displacement changes, the end-effector's deflection is compensated by adjusting the nominal joint positions.

CONCLUSIONS

The classical Timoshenko's beam theory and the Castigliano's second theorem used to calculate robotic link deflections are compared. It is found that the additional link deflections resulting from angular deflections significantly contribute the robot end-effector's deflection. The additional deflections are more accurately calculated using the Castigliano's second theorem. Experiments were carried out on a house-made planar two-link robot. As can be seen in Table III, with the consideration of the additional link deflections the theoretical calculations are generally in agreement with the experimental data. Although this study shows only the most significant vertical deflection data, the developed methodology can be used to find all of six deflection components.

It is also found that the end-effector's deflection heavily depends on the arm configuration. From the minimum deflection point of view, the configuration which produces the smallest deflection is considered as an optimum. The deflection is then compensated based on the selected optimum configuration. As shown in step 9 of the elbow manipulator example, configuration 6 (the optimum) is selected whose to-be-corrected joint angles are all less than 0.01 degrees. A practical problem arises when these angles are less than the resolutions of regular joint actuators. In this case, no compensation is necessary. Notice that configuration 7 produces a deflection almost 19 times as much as the configuration 6 does. If the configuration 7 were chosen, corrections in joint angles would be substantial.

Another consideration on selecting the arm configuration can be based on the so-called manipulator reliability developed by Bhatti and Rao.[12] The manipulator reliability was defined as the probability of end-effector's pose (position and orientation) falling within a specified range from the desired pose. If more than one arm configuration is possible to perform a certain task, the configuration which gives the highest reliability will be selected. The configuration thus selected may not be the same as that selected for producing a minimum deflection. This will be a decision-making problem for a robot user.

The authors would like to acknowledge the support of this work by the Ohio Institutional Research Challenge Program through the Cleveland State University.

References

1. D. E. Whitney, "Deflection and Vibration of Jointed Beams, Design and Control of Remote Manipulators," NASA Quarterly Report, CR-123795, July, 1972.
2. S. Derby, "The deflection and compensation of general purpose robot arms," *Mechanism and Machine Theory*, **18**, 445–450 (1983).
3. A. Zalucky and D. E. Hardt, "Active control of robot structure deflections," *Journal of Dynamic Systems, Measurement, and Control, Transactions of the ASME*, **106**, (1) (1984).
4. A. Maghdari and M. Shahinpoor, "Elastic deformation characteristics of PUMA 560 robot manipulator," *International Journal of Robotics and Automation*, **2**, 1–5 (1987).
5. R. G. Fenton and J. M. Reeder, "Motion planing for robots using an elastic deflection compensating algorithm," *International Journal of Robotics and Automation*, **2**, 1–5 (1987).
6. S. C. Tang and C. C. Wang, "Computation of the effects of link deflections and joint compliance on robot positioning," in *Proc. of the 1987 IEEE Conference on Robotics and Automation*, 1987, pp. 910–915.
7. D. E. Whitney, C. Lozinski, and J. Rourke, "Industrial robot forward calibration method and results," *Journal of Dynamic Systems, Measurement, and Control, Transactions of the ASME*, **108**, 1–8 (1986).
8. R. P. Paul, *Robot Manipulators: Mathematics, Programming, and Control*, The MIT Press, Cambridge, MA, 1986.
9. J. Denavit and R. S. Hartenberg, "A kinematic notation for lower-pair mechanisms based on matrices," *ASME Journal of Applied Mechanics*, June, 215–221 (1955).
10. S. P. Timoshenko and J. M. Gere, *Mechanics of Materials*, Van Nostrand Reinhold Company, 1971.
11. A. C. Ugural and S. K. Fenster, *Advanced Strength and Applied Elasticity*, Second Edition, Elsevier Science Publishing Co. Inc., 1987.
12. P. K. Bhatti and S. S. Rao, "Reliability analysis of robot manipulators," *ASME Journal of Mechanisms, Transmissions and Automation in Design*, **110**, 175–181 (1988).

APPENDIX: THE EXPRESSION OF THE TOTAL DEFLECTION AT THE END-EFFECTOR OF THE ELBOW MANIPULATOR

The total deflection, dy at the end-effector of the six-degree-of-freedom Elbow Manipulator is derived. It comprises two parts, dy_1 and dy_2, where dy_1 is the sum of the additional link deflections resulting from the angular deflections of all joints, and dy_2 is the sum of the link deflections calculated based on the Timoshenko's beam theory. The expression for the total deflection is as follows:

$$dy = dy_1 + dy_2$$

where

$$\begin{aligned}dy_1 = {} & A(a_2C_2 + 2a_3C_{23} + 3a_4C_{234} + 2d_6C_{234}S_5 + d_6S_{2345})/E_6I_6 \\ & - B(a_2C_2 + 2a_3C_{23} + 3a_4C_{234} + 3d_6C_{234}S_5)/E_4I_4 \\ & - C(a_2C_2 + 2a_3C_{23} + 2a_4C_{234} + 2d_6C_{234}S_5)/E_3I_3 \\ & - D(a_2C_2 + a_3C_{23} + a_4C_{234} + d_6C_{234}S_5)/E_2I_2\end{aligned}$$

where

$$\begin{aligned}A &= C_{234}C_5(3Pd_6^2 + W_6d_6^3)/6 \\ B &= [Pd_6 + (W_6d_6^2/2)]a_4C_{234}S_5 + (P + W_6d_6)a_4^2C_{234}/2 + W_6a_4^3C_{234}/6 \\ C &= [P + (W_6d_6/2)d_6a_3Ca_{234}S_5 + [P + (W_4a_4/2) + W_6d_6]a_3a_4C_{234} \\ &\quad + (P + W_4a_4 + W_6d_6)a_3^2C_{23}/2 + W_3a_3^3C_{23}/6 \\ D &= [(P + (W_6d_6/2)]a_2d_6C_{234}S_5 + [P + W_6d_6 + (W_4a_4/2)]a_2a_4C_{234} \\ &\quad + [P + W_6d_6 + W_4a_4 + (W_3a_3/2)]a_2a_3C_{23} \\ &\quad + (P + W_6d_6 + W_4a_4 + W_3a_3)a_2^2C_2/2 + W_2a_2^3C_2/6\end{aligned}$$

a_i and d_i are link parameters defined in Table IV; W_i, E_i and I_i are the weight, modulus of elasticity, and moment of inertia of the ith link, respectively. P is the applied load at the end-effector.

C_2 = Cosine of angle (θ_2)
C_{234} = Cosine of angle $(\theta_2 + \theta_3 + \theta_4)$
S_5 = Sine of angle (θ_5), . . . etc.

and dy_2 =

$$\begin{aligned}& - (Pd_6^3/3 - Pd_6^3S_{234}^2S_5^2/3 + W_6d_6^4/8 - W_6d_6^4S_{234}^2S_5^2/8)/E_6I_6 \\ & - (Pa_4^3C_{234}^2/3 - Pa_4^2d_6C_{234}^2S_5/2 + W_6a_4^3d_6C_{234}^2/3 \\ & \qquad - W_6a_4^2d_6^2C_{234}^2S_5/4 + W_4a_4^4C_{234}^2/8)/E_4I_4 \\ & - (Pa_3^3C_{23}^2/3 + Pa_3^2a_4C_{234}C_{23}/2 + Pa_3^2d_6C_{234}C_{23}S_5/2 \\ & \qquad + W_6a_3^3d_6C_{23}^2/3 + W_6a_3^2a_4d_6C_{234}C_3/2 + W_6a_3^2d_6^2C_{234}C_{23}S_5/4 \\ & \qquad + W_4a_3^3a_4C_{23}^2/3 + W_4a_3^2a_4^2C_{234}C_{23}/4 + W_3a_3^4C_{23}^2/8)/E_3I_3\end{aligned}$$

$$
\begin{aligned}
&- (Pa_2^3C_2^2/3 + Pa_2^2a_3C_{23}C_2/2 + Pa_2^2a_4C_{234}C_2/2 + Pa_2^2d_6C_{234}C_2S_5/2 \\
&\quad + W_6a_2^3d_6C_2^2/3 + W_6a_2^2a_3d_6C_{23}C_2/2 + W_6a_2^2a_4d_6C_{234}C_2/2 \\
&\quad + W_6a_2^2d_6^2C_{234}C_2S_5/4 + W_4a_2^3a_4C_2^2/3 + W_4a_2^2a_3a_4C_{23}C_2/2 \\
&\quad + W_4a_2^2a_4^2C_{234}C_2/4 + W_3a_2^3a_3C_2^2/3 + W_3a_2^2a_3^2C_{23}C_2/4 \\
&\quad + W_2a_2^4C_2^2/8)/E_2I_2
\end{aligned}
$$